ORIGINAL ARTICLE

Rest/stress myocardial perfusion imaging by positron emission tomography with ^{18}F-Flurpiridaz: A feasibility study in mice

Susan Bengs,[a,b] Geoffrey I. Warnock,[a,b] Angela Portmann,[a,b] Nidaa Mikail,[a,b] Alexia Rossi,[a,b] Hazem Ahmed,[c] Dominik Etter,[a,b] Valerie Treyer,[a] Livio Gisler,[c] Stefanie K. Pfister,[d] Caitlin V. M. L. Jie,[c] Alexander Meisel,[a,b] Claudia Keller,[c] Steven H. Liang,[d] Roger Schibli,[a,c] Linjing Mu,[a,c] Ronny R. Buechel,[a] Philipp A. Kaufmann,[a] Simon M. Ametamey,[c] Catherine Gebhard,[a,b] and Ahmed Haider[a,b,d]

[a] Department of Nuclear Medicine, University Hospital Zurich, Zurich, Switzerland
[b] Center for Molecular Cardiology, University of Zurich, Schlieren, Switzerland
[c] Institute of Pharmaceutical Sciences, ETH Zurich, Zurich, Switzerland
[d] Division of Nuclear Medicine and Molecular Imaging, Massachusetts General Hospital & Department of Radiology, Harvard Medical School, Boston, MA

Background. Myocardial perfusion imaging by positron emission tomography (PET-MPI) is the current gold standard for quantification of myocardial blood flow. ^{18}F-flurpiridaz was recently introduced as a valid alternative to currently used PET-MPI probes. Nonetheless, optimum scan duration and time interval for image analysis are currently unknown. Further, it is unclear whether rest/stress PET-MPI with ^{18}F-flurpiridaz is feasible in mice.

Methods. Rest/stress PET-MPI was performed with ^{18}F-flurpiridaz (0.6-3.0 MBq) in 27 mice aged 7–8 months. Regadenoson (0.1 µg/g) was used for induction of vasodilator stress. Kinetic modeling was performed using a metabolite-corrected arterial input function. Image-derived myocardial ^{18}F-flurpiridaz uptake was assessed for different time intervals by placing a volume of interest in the left ventricular myocardium.

Results. Tracer kinetics were best described by a two-tissue compartment model. K_1 ranged from 6.7 to 20.0 mL·cm^{-3}·min^{-1}, while myocardial volumes of distribution (V_T) were between 34.6 and 83.6 mL·cm^{-3}. Of note, myocardial ^{18}F-flurpiridaz uptake (%ID/g) was significantly correlated with K_1 at rest and following pharmacological vasodilation for all time intervals assessed. However, while Spearman's coefficients (r_s) ranged between 0.478 and 0.681, R^2 values were generally low. In contrast, an excellent correlation of myocardial ^{18}F-flurpiridaz uptake with V_T was obtained, particularly when employing the averaged myocardial uptake from 20 to 40 min post tracer injection ($R^2 \geq 0.98$). Notably, K_1 and V_T were similarly sensitive to pharmacological vasodilation induction. Further, mean stress-to-rest ratios of K_1, V_T, and %ID/g

^{18}F-flurpiridaz were virtually identical, suggesting that %ID/g ^{18}F-flurpiridaz can be used to estimate coronary flow reserve (CFR) in mice.

Conclusion. Our findings suggest that a simplified assessment of relative myocardial perfusion and CFR, based on image-derived tracer uptake, is feasible with ^{18}F-flurpiridaz in mice, enabling high-throughput mechanistic CFR studies in rodents. (J Nucl Cardiol 2023;30:62–73.)

Key Words: Rest/stress myocardial perfusion imaging (MPI) • positron emission tomography (PET) • ^{18}f-flurpiridaz • kinetic modeling • regadenoson • coronary artery disease (CAD) • microvascular dysfunction • myocardial ischemia • small animal PET • logan graphical analysis • tissue compartment model

INTRODUCTION

In the past two decades, the diagnosis of coronary artery disease (CAD) has undergone a remarkable evolution from conventional anatomical assessment of coronary arteries to an integral diagnostic approach combining anatomical and functional cardiovascular imaging modalities. Although coronary computed tomography angiography (CCTA) remains the first-line diagnostic tool for patients with suspected CAD,[1] a significant proportion of patients presenting with angina show no evidence of epicardial stenosis[2] and may suffer from a condition called INOCA (ischemia with no obstructive coronary arteries) caused by vasospastic disorders or microvascular dysfunction.[3] The latter is associated with a reduced coronary flow reserve (CFR) and can be quantified by rest/stress myocardial perfusion imaging (MPI) with positron emission tomography (PET). As such, PET-MPI has shown a high diagnostic accuracy and independent prognostic value in INOCA patients.[4] Further, a recent meta-analysis revealed that a reduced CFR was associated with an increased risk of cardiovascular and all-cause mortality across multiple disease populations, including patients with acute and chronic coronary syndromes, heart failure, aortic stenosis, heart transplant, and systemic sclerosis, demonstrating the versatile use of CFR in cardiovascular medicine.[5]

^{18}F-flurpiridaz has recently been introduced as a novel radiofluorinated probe for PET-MPI.[6–8] Despite the excellent performance characteristic of ^{18}F-flurpiridaz, the physical half-life of 109.8 minutes constitutes a major challenge for efficient rest/stress testing protocols. Indeed, conventional 1-day protocols, as they are routinely performed with rubidium-82, ^{13}N-ammonia or ^{15}O-water, are hampered by the residual myocardial radioactivity from the initial ^{18}F-flurpiridaz injection, which affects the time-activity curves (TACs) obtained after the second ^{18}F-flurpiridaz injection. Indeed, several unanswered questions remain regarding the ideal scan duration with ^{18}F-flurpiridaz, as well as the most accurate time frame post injection for the assessment of myocardial perfusion and CFR. Further, given the widespread

use of CAD mouse models, the feasibility of rest/stress PET-MPI with ^{18}F-flurpiridaz in mice would ultimately allow the assessment of molecular determinants affecting myocardial perfusion and CFR in these disease models.

The aim of the study was (1) to identify the optimal time frame for PET imaging following ^{18}F-flurpiridaz injection and (2) to assess whether a simplified and image-derived model would allow sequential rest and stress PET-MPI, thereby providing accurate information on myocardial perfusion and CFR in mice.

METHODS

Animals

Animal care and experimental procedures were performed in accordance with the Swiss Animal Welfare legislation and approved by the Veterinary Office of the Canton Zurich, Switzerland. Female and male FVB/N mice (N = 27, 14 females) were obtained from Janvier Labs (Le Genest-Saint-Isle, France), kept with free access to food and water and were scanned at the age of 7–8 months.

Study protocol and image acquisition

^{18}F-Flurpiridaz radiolabeling and precursor synthesis were reported elsewhere.[9–11] PET/CT was performed in animals that were anaesthetized using 1.3–2.0% isoflurane in oxygen-enriched air (1:1). Depth of anesthesia was monitored via respiratory rate measurement (SA Instruments, Inc., Stony Brook, USA). Body temperature was monitored using a rectal probe and was kept at 37°C with a temperature-adjusted air stream. A dose of 0.6-3.0 MBq ^{18}F-flurpiridaz was administered via tail-vein injection 60 sec after the start of the PET scan. Tracer distribution was recorded in dynamic PET acquisition mode over a time period of 41 min, before a bolus of regadenoson (0.1 $\mu g \cdot g^{-1}$) and a second dose of ^{18}F-flurpiridaz (2.2-8.1 MBq) were injected via a preinstalled intravenous catheter. PET imaging was performed with a calibrated Super Argus PET/CT scanner

(Sedecal, Spain) with an axial field of view of 4.8 cm and a spatial resolution of 1.6-1.7 mm in full width at half-maximum,[12,13] followed by a CT scan for anatomical information. PET data reconstruction was carried out using the manufacturer's 2D iterative (OSEM, ordered subset expectation maximization, 2 iterations, 16 subsets) algorithm, and corrections for dead time, decay, scatter, and attenuation, at a voxel size of 0.3875 x 0.3875 x 0.775 mm³. All radioactivities were decay-corrected to the time of tracer injection.

Image analysis and generation of rest/stress time-activity curves

Reconstructed PET data were processed with PMOD v.3.8 (PMOD Technologies Ltd., Switzerland) via manual delineation of the myocardium to generate volumes of interest (VOIs) and respective time-activity curves. Decay-corrected time-activity curves were calculated for the myocardium VOI either as kBq/cc or % injected dose per gram tissue (%ID/g). An exponential model was fitted for each rest scan to estimate the radioactivity that remained in the myocardium at 41 to 82 min post injection from the initial ^{18}F-flurpiridaz injection (Figure 1A, extrapolation curve). To obtain the corrected time-activity curves following stress injection (Figure 1A, ^{18}F-flurpiridaz and regadenoson), extrapolation curves were subtracted from the respective image-derived time-activity curves at 41 to 82 min post injection. Correction for the injected dose yielded the final rest and stress time-activity curves (Figure 1B).

Input function

An arteriovenous shunt and portable coincidence detector (twilite, swisstrace, Menzingen, Switzerland) were used to record the tracer concentration in the blood by continuous sampling and simultaneously with the PET data acquisition in five FVB/N mice (30.1–32.6 g). The coincidence detector was cross-calibrated to the PET for kBq/cc output. The delay between tissue and blood time-activity curves was determined as part of the model fitting procedure, and the final input function was corrected for plasma metabolites and plasma-to-blood ratio (Supplemental Information). Metabolite-corrected input functions were used for all analyses. The resulting five input functions were averaged, and the average was used as a surrogate input function for all animals scanned without arteriovenous shunt system (Supplemental Information).

Kinetic modeling Kinetic modeling was performed with the PKIN tool of PMOD v.3.8 (PMOD Technologies Ltd., Switzerland). The kinetics of ^{18}F-flurpiridaz was evaluated with a one- and two-tissue compartment model using the following equations:

One-tissue compartment model:

$$\frac{dC_1}{dt} = K_1 C_p(t) - k_2 C_1(t) \qquad (1)$$
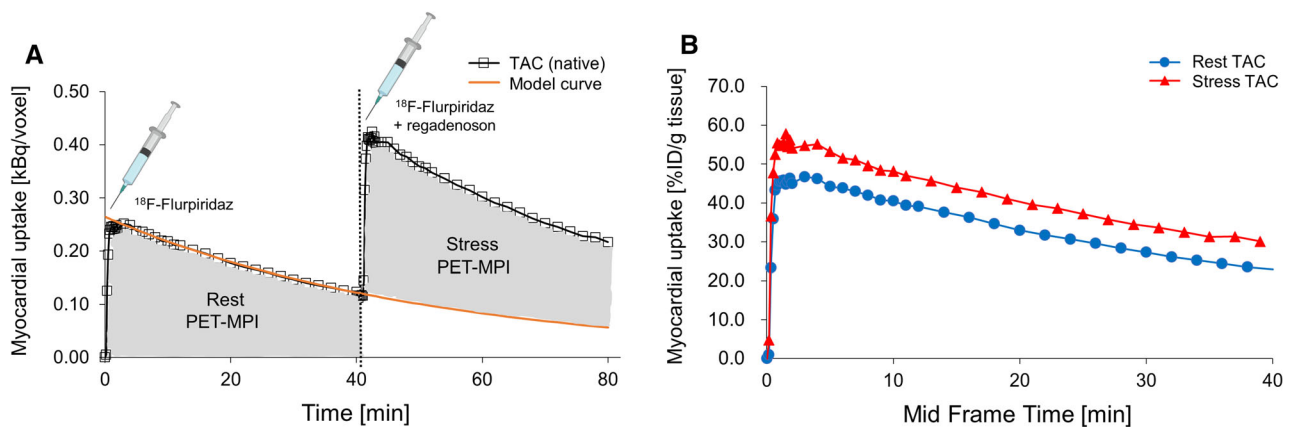
$$C_{Model}(t) = (1 - v_b)C_1(t) + v_b C_b(t) \qquad (2)$$

Figure 1. Time-activity curves (TACs) of the mouse myocardium upon tail-vein injections of ^{18}F-flurpiridaz. (**A**). Native TACs after rest (^{18}F-flurpiridaz) and stress (^{18}F-flurpiridaz + regadenoson) injection, presented as kBq per voxel. The model curve was fitted with a single exponential model to subtract ^{18}F-flurpiridaz injection 1 from injection 2. (**B**) Final rest and stress TACs after correction for injected ^{18}F-flurpiridaz dose, presented as percent injected dose per gram tissue (%ID/g). Note that the correction of the stress curve was performed prior to the normalization to the injected dose.

Two-tissue compartment model:

$$\frac{dC_1}{dt} = K_1 C_{\mathrm{p}}(t) - (k_2 + k_3)C_1(t) + k_4 C_2(t) \quad (3)$$

$$\frac{dC_2}{dt} = k_3 C_1(t) - k_4 C_2(t) \quad (4)$$

$$C_{\mathrm{Model}}(t) = (1 - v_{\mathrm{b}}) \times (C_1(t) + C_2(t)) + v_{\mathrm{b}} \times C_{\mathrm{b}}(t) \quad (5)$$

$$V_T = K_1 * \frac{\left(1 + \frac{k_3}{k_4}\right)}{k_2} \quad (6)$$

$C_{\mathrm{p}}(t)$ is the input function, $C_1(t)$ and $C_2(t)$ are the concentrations in the first and second tissue compartments. K_1 [mL·cm^{-3}·min^{-1}] and k_2 [1 min^{-1}] represent the uptake and clearance rates from the plasma to the first tissue compartment, whereas k_3 [1 min^{-1}] and k_4 [1 min^{-1}] are the rate constants describing the exchange between the first and second tissue compartment. $C_{\mathrm{Model}}(t)$ shows the operational model curve, with the concentration $C_{\mathrm{b}}(t)$ in the whole blood, and the blood volume fraction v_{b}, which was set to 0.13, as previously reported for the myocardium.[14] Tissue distribution volume (V_{T}) was calculated from the fit K_1 and apparent rate constants k_2, as well as k_3 and k_4 according to Eq. 6, and was additionally assessed by graphical Logan analysis.[15]

Statistics

Continuous variables are presented as mean ± standard error of the mean (SEM). Student's t test and analysis of variance (ANOVA) tests were used for group comparisons of continuous variables. For multiple comparisons, Bonferroni correction was applied. Strength and direction of associations were assessed by Spearman's rank-order correlation (r_{s}). Outliers were assessed based on the Grubb's test.[16] A two-tailed P value of $\leq$ 0.05 was deemed statistically significant. Statistical analyses were carried out with SPSS (SPSS Statistics for Windows Version 24.0. IBM Corp. Armonk, NY).

RESULTS

Rest/stress myocardial perfusion imaging

Time-activity curves (TACs) of ^{18}F-flurpiridaz in the myocardium are depicted in Figure 1. At initial ^{18}F-flurpiridaz injection, a rapid myocardial tracer inflow was observed, followed by a slow washout. Preliminary experiments revealed that a scan time of 40 min was sufficient to obtain accurate fits for the terminal washout phase (Figure 1A, model curve), thus allowing to account for residual myocardial activity from the initial ^{18}F-flurpiridaz injection. Details on model curve fitting

are given in the Supplemental Information. Subtraction of the extrapolated model curves from respective native TACs at 40-80 min post injection and correction for the injected ^{18}F-flurpiridaz dose yielded the final stress TACs (Figure 1B). Notably, myocardial TACs were higher for the stress than for the rest scans at every measured time point, indicating a sustained increase of myocardial ^{18}F-flurpiridaz uptake following regadenoson injection (Figure 1B). The increase of myocardial ^{18}F-flurpiridaz uptake under pharmacological vasodilation conditions was visually confirmed by PET images of the mouse myocardium (Supplemental Information).

Quantification of absolute myocardial blood flow by kinetic modeling

To determine absolute myocardial blood flow (MBF), we employed kinetic tracer modeling using a metabolite-corrected input function that was recorded by continuous arterial blood sampling. Results of kinetic modeling were compared for one- and two-tissue compartment models. While the kinetic results were satisfactory by visual inspection for the two-tissue compartment model (Figure 2), the one-tissue compartment model did not provide accurate fitting. Along this line, a comparison of ''goodness-of-fit'' parameters such as the Akaike information criterion (AIC), Schwartz criterion (SC), Model selection criterion (MSC), and R^2 consistently confirmed that the two-tissue compartment model was the superior model (Supplemental Information). K_1, which is typically considered a measure of absolute MBF for tracers with high myocardial extraction fraction such as ^{18}F-flurpiridaz,[8] ranged from 6.7 to 20.0 mL·cm^{-3}·min^{-1}, while myocardial V_T values between 34.6 and 83.6 mL/cm^3 were obtained. A representative example of the two-tissue compartment model fit is shown in Figure 2B. V_{T} values obtained from Logan graphical analysis were in agreement with the two-tissue compartment model fit (Figure 2C). These results suggest that the two-tissue compartment model constitutes a suitable model for the assessment of ^{18}F-flurpiridaz kinetic parameters in mice, which is in agreement with previous studies in pigs and humans.[17–19]

Correlation of myocardial ^{18}F-flurpiridaz uptake with K_1 and V_T

In a next step, we sought to assess whether the image-derived myocardial tissue uptake of ^{18}F-flurpiridaz (%ID/g tissue) can be used as a surrogate measure for relative myocardial perfusion changes. Myocardial ^{18}F-flurpiridaz uptake was significantly correlated with K_1 from two-tissue compartment modeling. As shown in
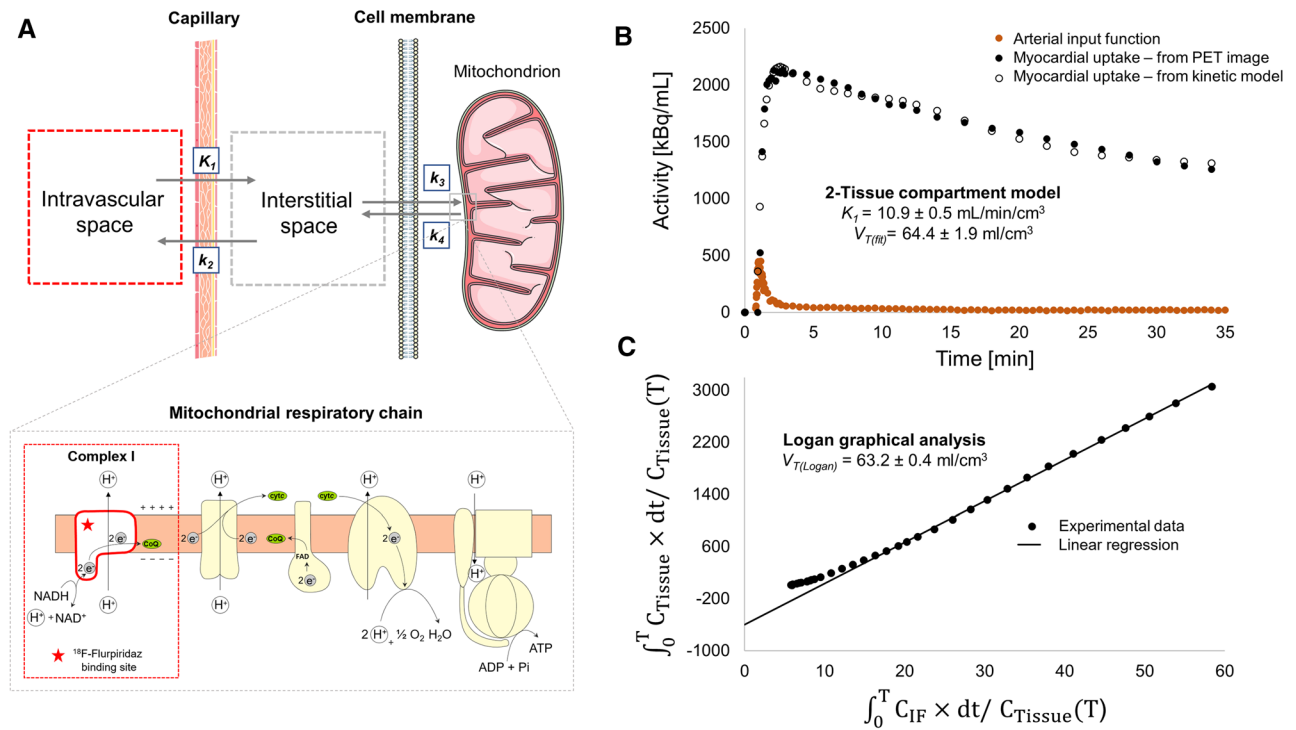
Figure 2. Two-tissue compartment model for ^{18}F-flurpiridaz in the mouse myocardium. (**A**) Visualization of the model. While K_1 and k_2 describe tracer delivery to the myocardium and clearance from the myocardium, respectively, k_3 and k_4 represent the association and dissociation rate constants toward mitochondrial complex I (MC-I), which is located at the mitochondrial membrane of cardiomyocytes. (**B**) Representative two-tissue compartment fitting for the assessment of K_1 and tissue volume of distribution (V_T). (**C**) Representative logan graphical analysis.

Table 1. Correlation of image-derived myocardial ^{18}F-flurpiridaz uptake with perfusion constant K_1 at resting state (n = 27)

Time	0-2 min	2-7 min	7-11 min	11-20 min	20-40 min	0-40 min
r (Spearman)	0.573	0.495	0.490	0.478	0.509	0.509
P value	0.002	0.009	0.009	0.012	0.007	0.007
R^2	0.24	0.20	0.21	0.21	0.21	0.23

Table 2. Correlation of image-derived myocardial ^{18}F-flurpiridaz uptake with perfusion constant K_1 following regadenoson injection (n = 27)

Time	0-2 min	2-7 min	7-11 min	11-20 min	20-40 min	0-40 min
r (Spearman)	0.672	0.681	0.676	0.671	0.617	0.668
P value	< 0.001	< 0.001	< 0.001	< 0.001	< 0.001	< 0.001
R^2	0.43	0.42	0.41	0.38	0.33	0.41

Tables 1 and 2, Spearman's coefficients (r_s) ranged between 0.478 and 0.573 for the rest scans and were higher after regadenoson injection (0.617-0.681), whereas significant correlations were obtained for all tested time slots. Nonetheless, R^2 values were generally low, ranging from 0.21 to 0.43, which indicates that K_1 does not sufficiently explain a large proportion of the variability in image-derived myocardial ^{18}F-flurpiridaz uptake.

In contrast, when myocardial ^{18}F-flurpiridaz uptake was compared to the respective volumes of distribution (V_T), excellent correlations were obtained between %ID/g tissue and V_T at rest (Figure 3). Notably, it was found that the two-tissue compartment model described the myocardial ^{18}F-flurpiridaz uptake most accurately at later time frames (rest scans: Figure 3C, 7-11 min post injection, $R^2 = 0.98$, Figure 3D, 11-20 min post injection, $R^2 = 0.99$, and Figure 3E, 20-40 min post injection, $R^2 = 0.99$), while earlier time frames were associated with lower R^2 values (Figure 3A, 0-2 min post injection $R^2 = 0.71$; Figure 3B, 2–7 min post injection, $R^2 = 0.95$). Similarly, the correlation model between %ID/g tissue and V_T was superior at later time frames following regadenoson injection, as depicted in Figure 4. Overall, %ID/g tissue, averaged from 20 to 40

min post injection, was most accurately described by the two-tissue compartment model under rest conditions and following pharmacological vasodilation.

Coronary Flow Reserve CFR can be calculated from the ratio of MBF during regadenoson-induced vasodilation to the MBF under resting conditions.[20] Given that K_1 constitutes a measure of absolute MBF, we used the ratio of K_1 following regadenoson injection to K_1 at resting condition to calculate the CFR. As expected, K_1 was significantly higher following regadenoson injection (Figure 5A, $P < 0.001$). Similarly, regadenoson-induced coronary vasodilation led to a significant increase in V_T (Figure 5B, $P < 0.001$). The resulting mean stress-to-rest ratios for K_1 and V_T were identical (Figure 5C, 1.41±0.29 vs 1.41±0.17, $P = 0.92$), however, with a higher variability obtained for K_1. These results support the concept that both, K_1 and V_T, are similarly sensitive to pharmacologically induced changes of MBF in mice, while V_T seems to constitute a more robust parameter for the estimation of CFR. Notably, it was found that stress-to-rest ratios of image-derived myocardial ^{18}F-flurpiridaz uptake accurately predicted CFR, as depicted in Figure 6. While tracer washout led to a gradual reduction of averaged %ID/g tissue over time, under resting conditions
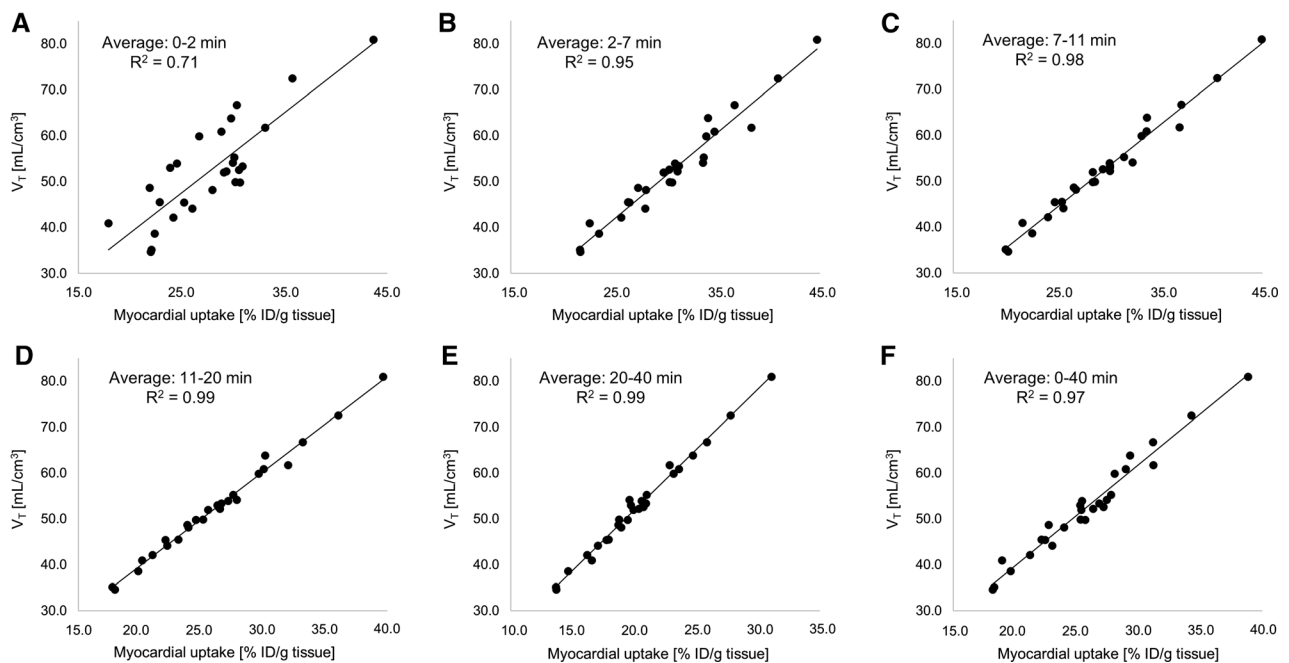

Figure 3. Resting state (no regadenoson) correlations of image-derived myocardial ^{18}F-flurpiridaz uptake (%ID/g tissue), averaged at different time intervals, with tissue volume of distribution (V_T). Early time intervals revealed lower R^2 values, while later time intervals reached an R^2 value of up to 0.99, indicating an excellent correlation between V_T and %ID/g tissue ^{18}F-flurpiridaz. Averaged time intervals included (**A**) 0-2 min, (**B**) 2-7 min, (**C**) 7-11 min, (**D**) 11-20 min, (**E**) 20-40 min and (**F**) 0-40 min post injection.
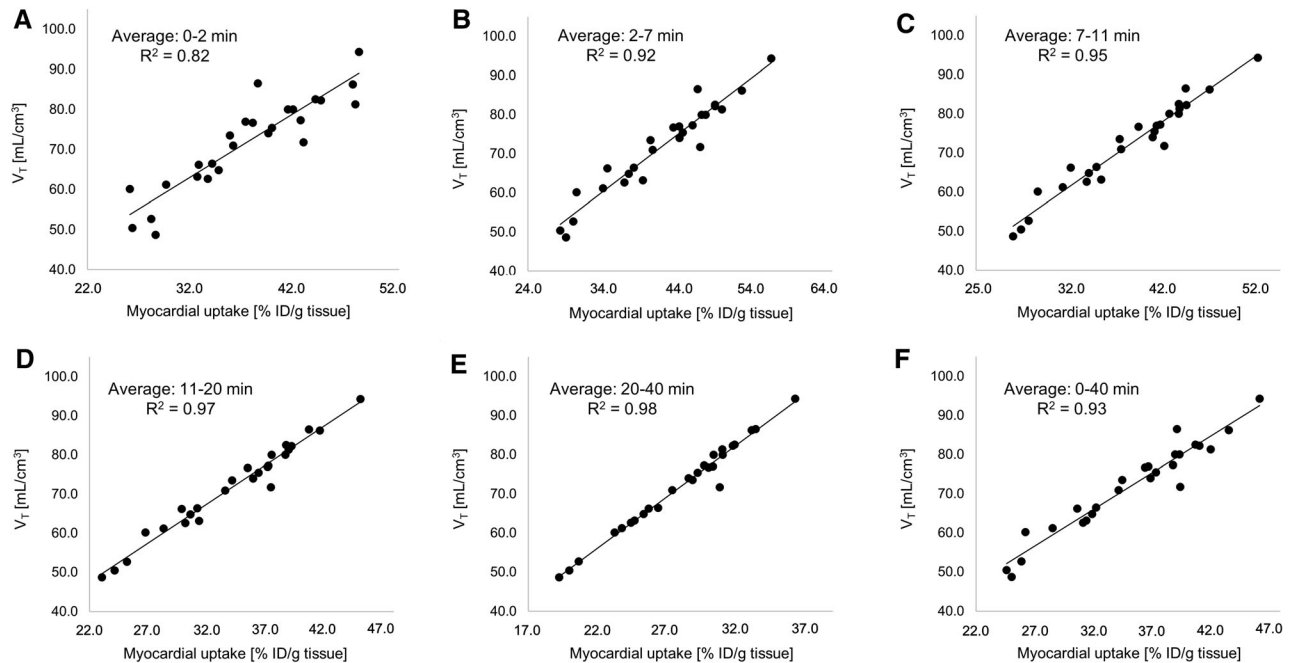
Figure 4. Correlations of image-derived myocardial ^{18}F-flurpiridaz uptake (%ID/g tissue) following regadenoson-induced stress, with tissue volume of distribution (V_T). Early time intervals revealed lower R^2 values, while later time intervals reached an R^2 value of up to 0.98, indicating an excellent correlation between V_T and %ID/g tissue ^{18}F-flurpiridaz. Averaged time intervals included (**A**) 0-2 min, (**B**) 2-7 min, (**C**), 7-11 min, (**D**) 11-20 min, (**E**) 20-40 min and (**F**) 0-40 min post injection.
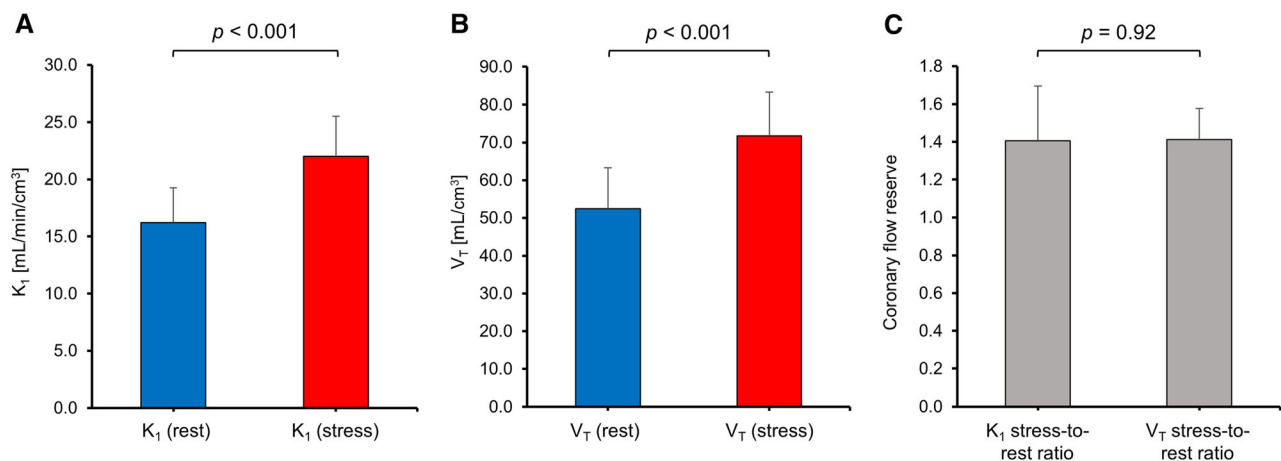

Figure 5. Average K_1 and V_T under resting conditions and following pharmacological stress testing. (**A**) K_1 was significantly higher following regadenoson administration ($P < 0.001$). (**B**) V_T was significantly elevated following regadenoson administration ($P < 0.001$). (**C**) Mean coronary flow reserve estimated from stress-to-rest ratios of K_1 and V_T.

(Figure 6A) and following regadenoson injection (Figure 6B), the stress-to-rest ratio did not differ significantly between time intervals (Figure 6C). With a mean stress-to-rest ratio of 1.40±0.20, %ID/g ^{18}F-flurpiridaz from 20 to 40 min post injection provided the most accurate mean ratio, as compared to CFR determined from K_1 by the two-tissue compartment model.
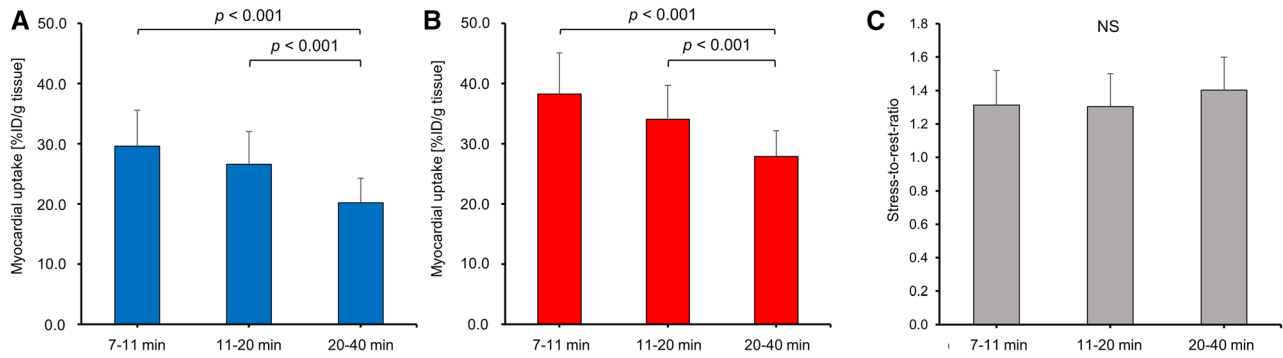
Figure 6. Myocardial ^{18}F-flurpiridaz uptake averaged from 7-11, 11-20 and 20-40 min post injection. A significant reduction of averaged %ID/g tissue of ^{18}F-flurpiridaz was found toward later time intervals (**A**) at resting state as well as (**B**) following pharmacological stress testing. (**C**) In contrast, stress-to-rest ratios did not significantly differ between different time intervals.

Discussion In the present study, we show that rest/stress MPI with ^{18}F-flurpiridaz in mice follows a two-tissue compartment model. While K_1 and V_T were both similarly sensitive to vasodilator-induced increase of MBF, V_T exhibited a superior correlation with image-derived myocardial tracer uptake at all measured time intervals. In particular, image-derived tracer uptake at later time intervals revealed ideal coefficients of determination (R^2 up to 0.99) when correlated with V_T. Further, the average stress-to-rest ratio of myocardial tracer uptake (%ID/g tissue), obtained from 20 to 40 min post injection, was identical to the stress-to-rest ratios of K_1 and V_T. These results suggest that myocardial ^{18}F-flurpiridaz uptake (%ID/g) in mice, as determined from dynamic PET, correlates with MBF and can be used to estimate relative myocardial perfusion changes as well as CFR when pharmacological vasodilation is employed.

To the best of our knowledge, this is the first study to assess the feasibility of rest/stress PET-MPI with ^{18}F-flurpiridaz in mice. In agreement with previous reports in other species, including pigs[21] and humans,[19] we found that a two-tissue compartment model was suitable to predict ^{18}F-flurpiridaz uptake in the mouse myocardium. Nonetheless, significant species differences were observed with regard to tracer washout from the myocardium. While myocardial ^{18}F-flurpiridaz washout was negligible in pigs and humans, our time-activity curves unveiled a demonstrably faster kinetics in mice with evident washout from the mouse myocardium starting at 5–10 min post injection.[19,21] Our results point toward species differences in myocardial tracer retention that need to be taken into consideration for kinetic modeling. As such, while k_4 (dissociation rate constant) was manually set to zero in previous studies

with other species,[17,21,22] we did not employ any restrictions for k_4 in mice. Of note, a fast decline of the parent tracer fraction was detected in the mouse plasma following tail-vein injection of ^{18}F-flurpiridaz (Supplemental Information), which might, at least in part, explain the observed species differences in tracer washout from the myocardium. To account for the metabolic degradation, we used metabolite-corrected input functions for all animals tested. By *ex vivo* metabolite analysis, the myocardium was found to show an intact parent fraction of $> 99\%$, suggesting that the contribution of radiometabolites to the overall myocardial radioactivity was negligible. In contrast to the two-tissue compartment model, the one-tissue compartment model did not result in satisfactory results by visual inspection and assessment of different model fit indicators, suggesting that binding to MC-I has a significant contribution to the kinetics as well as perfusion-linked ^{18}F-flurpiridaz delivery to the mouse myocardium.

Due to the availability of rubidium-82 generators, which obviates the need for a cyclotron, rubidium-82 is the most frequently used probe for PET-MPI. Nonetheless, the relatively high positron range results in an inferior spatial resolution, as compared to other PET isotopes.[23] In contrast, ^{15}O-water and ^{13}N-ammonia exhibit superior spatial resolutions to rubidium-82 and are validated perfusion tracers; however, their short physical half-lives do not allow satellite distribution, thus, rendering an on-site cyclotron indispensable.[21] Efforts to develop a radiofluorinated myocardial perfusion tracer with increased physical half-life and spatial resolution have ultimately led to the discovery of ^{18}F-flurpiridaz.[6–8] Unlike other probes for PET-MPI, ^{18}F-flurpiridaz binds to the mitochondrial complex I (MC-I), which is highly abundant in cardiomyocytes.[8,21] The

latter allows selective visualization of the myocardium, providing remarkably high signal-to-background ratios and thus high image quality.[9,24–30] In experimental models, ^{18}F-flurpiridaz exhibited a relatively high myocardial extraction fraction of 0.94, which was consistent at different flow rates, and demonstrated favorable performance characteristics as a myocardial perfusion tracer.[7,8,17,27,31–34] Notably, we observed that peak arterial radioactivity was lower than peak myocardial activity across all animals tested, which might be explained by the relatively high first-pass myocardial extraction fraction of ^{18}F-flurpiridaz.

Despite the reported favorable properties of ^{18}F-flurpiridaz for PET-MPI, the sustained myocardial radioactivity from the initial scan may affect the time-activity curves upon the second injection—particularly if rest and stress scans are performed on the same day. In our study, pilot experiments were conducted to determine the minimum scan duration required to allow adequate extrapolation of the terminal phase via nonlinear regression models. Employing these models, we were able to correct for the residual myocardial radioactivity from the first ^{18}F-flurpiridaz injection. In light of the observed species differences in ^{18}F-flurpiridaz clearance from the myocardium, we conclude that a careful evaluation of the terminal phase for the underlying test species seems crucial for 1-day rest/stress PET-MPI protocols with ^{18}F-flurpiridaz.

Absolute MBF quantification has proven its utility in clinical routine; however, the latter requires an arterial input function[35] that can be derived from the PET image by placing a VOI in the left ventricular cavity.[36] While image-derived input functions are routinely obtained in clinical PET-MPI, this approach is hampered in mice due to the relatively small left ventricular dimensions. Accordingly, quantification of absolute MBF in mice requires arterial blood sampling, which is associated with significant technical challenges. To circumvent this limitation, we assessed whether myocardial ^{18}F-flurpiridaz uptake can be used to provide information on myocardial perfusion changes as well as fundamental kinetic parameters such as K_I and V_T. Indeed, although correlations of K_I with image-derived myocardial ^{18}F-flurpiridaz uptake were significant, R^2 values were generally below 0.5, indicating a poor fit for all time frames investigated. In contrast, ideal fits were obtained for the correlation of V_T with myocardial ^{18}F-flurpiridaz uptake, particularly at later time intervals such as 20–40 min post injection. Although K_I is closely linked to perfusion, our results suggest that the rapid tracer kinetics renders myocardial ^{18}F-flurpiridaz uptake more highly weighted toward MC-I binding than absolute MBF in mice. Further, early time intervals, which are critical for the accurate estimation of K_I, are

particularly susceptible to spillover effects from the blood pool as well as variability in manual injection time and potential animal distress that resulted from the injection procedure. Accordingly, the relation between K_I and myocardial ^{18}F-flurpiridaz uptake did not allow the prediction of absolute values for MBF from myocardial ^{18}F-flurpiridaz uptake in our study. Notably, however, %ID/g ^{18}F-flurpiridaz was highly correlated with V_T. Indeed, our findings suggested that V_T was reliably estimated from myocardial ^{18}F-flurpiridaz uptake in the absence of an arterial input function. Given (1) that V_T is sensitive to changes in K_I according to Eq. 6 and (2) that mean rest-to-stress ratios were comparable for V_T and K_I, it appears that changes in myocardial perfusion were accurately reflected by the model microparameter V_T. Accordingly, although %ID/g ^{18}F-flurpiridaz was not suitable to estimate values for absolute MBF, our data indicate that %ID/g ^{18}F-flurpiridaz can be used for intra- and interindividual comparisons of relative myocardial perfusion in mice. Further, mean CFR values were comparable when calculated from stress-to-rest ratios of K_I, V_T, and %ID/g ^{18}F-flurpiridaz from 20 to 40 min post injection, suggesting that stress-to-rest ratios of %ID/g ^{18}F-flurpiridaz can be used as a surrogate of CFR when pharmacological vasodilation is employed. In contrast to pharmacological vasodilation, however, it should be noted that the assessment of CFR from exercise stress testing is not recommended in the absence of an input function, particularly due to the substantial increase of cardiac output under exercise testing, which leads to a proportional dilution of the intravenous radiotracer dose.[37,38]

There are study limitations that should be pointed out. First, the lack of a reference standard to validate PET-MPI findings in mice constitutes a limitation of this study. Indeed, the assessment of CFR by PET-MPI in mice is a major challenge in contemporary cardiovascular research and studies of CFR by rest/stress MPI using PET in rodents are scarce in general. Although the spatial resolution of our PET scanner was in the range of reported left ventricular thickness < 1.8 mm for mice,[39] the positron ranges of conventional PET-MPI probes such as rubidium-82, ^{15}O-water, and ^{13}N-ammonia would not allow a sufficient spatial resolution for the assessment of CFR in the small mouse heart.[40] Conversely, the availability of a radiofluorinated probe now provides new perspectives for PET-MPI in mice and the fact that myocardial ^{18}F-flurpidaz uptake correlated well with K_I and V_T from quantitative kinetic modeling with an invasive metabolite-corrected input function is particularly encouraging. Second, high isoflurane concentrations can prompt coronary vasodilation and may have affected outcome measures of our study.[41]

However, previous work has shown that heart rate and mean systolic blood pressure remain stable at isoflurane concentration up to 2.0% in mice.[42,43] To minimize the vasodilatory properties of isoflurane, its concentration was kept at or below 2.0% throughout the entire experiment. Nonetheless, a vasodilatory effect of isoflurane cannot be completely ruled out in the present study. Third, an experimental arterial input function was only available in five animals, and the average of all five input functions was used as a population (surrogate) input function for kinetic modeling in animals without arterial shunt, as previously reported.[44] However, a linear regression analysis revealed that K_1 and V_T obtained from the surrogate input function and the respective input functions from shunt surgery were in good agreement (Supplemental Information). While obtaining an image-derived input function in mice is particularly challenging and prone to error, the approach of a surrogate input function constitutes a valid alternative for high-throughput studies.

In conclusion, our results indicate that ^{18}F-flurpiridaz can be used for rest/stress myocardial perfusion imaging in mice and follows a two-tissue compartment model. Myocardial ^{18}F-flurpiridaz uptake was equally sensitive to vasodilator stress as K_1 and V_T, suggesting that a simplified assessment of CFR, based on image-derived findings, is feasible when pharmacological vasodilation is employed. Further, although arterial blood sampling is required for absolute quantification of MBF, myocardial ^{18}F-flurpiridaz uptake can be used for relative comparison of myocardial perfusion in mice.

NEW KNOWLEDGE GAINED

In the present study, we show that rest/stress myocardial perfusion imaging in mice is feasible with ^{18}F-flurpiridaz and follows a two-tissue compartment model. Critical kinetic modeling parameters such as K_1 and V_T were sensitive to vasodilator-induced increase of myocardial blood flow. Further, the average stress-to-rest ratio of myocardial tracer uptake from 20 to 40 min post injection was identical to the stress-to-rest ratios of K_1 and V_T, indicating that myocardial ^{18}F-flurpiridaz uptake can be used to estimate relative myocardial perfusion changes and coronary flow reserve (CFR) in mice. The translational relevance of this study lies in the detrimental implications of an abnormal CFR in coronary artery disease (CAD) patients. The present findings encourage a wider use of PET-MPI for the assessment of CFR in mouse models of CAD, and pave the way for mechanistic studies that aim at identifying molecular variables affecting CFR.

Declarations

Disclosures

Open Access

References

1. Knuuti J, Wijns W, Saraste A, Capodanno D, Barbato E, Funck-Brentano C. 2019 ESC Guidelines for the diagnosis and management of chronic coronary syndromes: The Task Force for the diagnosis and management of chronic coronary syndromes of the European Society of Cardiology (ESC). Eur Heart J 2019;41:407-77.
2. Crea F, Camici PG, Bairey Merz CN. Coronary microvascular dysfunction: An update. Eur Heart J 2014;35:1101-11.
3. Camici PG, Crea F. Microvascular angina: a women's affair? Circ Cardiovasc Imaging 2015;8:3252.
4. Danad I, Raijmakers PG, Driessen RS, Leipsic J, Raju R, Naoum C, et al. Comparison of coronary CT angiography, SPECT, PET, and hybrid imaging for diagnosis of ischemic heart disease determined by fractional flow reserve. JAMA Cardiol 2017;2:1100-7.
5. Kelshiker MA, Seligman H, Howard JP, Rahman H, Foley M, Nowbar AN, et al. Coronary flow reserve and cardiovascular

outcomes: a systematic review and meta-analysis. Eur Heart J 2021;2021:775.

6. Huisman MC, Higuchi T, Reder S, Nekolla SG, Poethko T, Wester HJ, et al. Initial characterization of an 18F-labeled myocardial perfusion tracer. J Nucl Med 2008;49:630-6.

7. Yu M, Guaraldi MT, Mistry M, Kagan M, McDonald JL, Drew K, et al. BMS-747158-02: A novel PET myocardial perfusion imaging agent. J Nucl Cardiol 2007;14:789-98.

8. Yalamanchili P, Wexler E, Hayes M, Yu M, Bozek J, Kagan M, et al. Mechanism of uptake and retention of F-18 BMS-747158-02 in cardiomyocytes: A novel PET myocardial imaging agent. J Nucl Cardiol 2007;14:782-8.

9. Purohit A, Radeke H, Azure M, Hanson K, Benetti R, Su F, et al. Synthesis and biological evaluation of pyridazinone analogues as potential cardiac positron emission tomography tracers. J Med Chem 2008;51:2954-70.

10. Yalamanchili P, Wexler E, Hayes M, Yu M, Bozek J, Kagan M, et al. Mechanism of uptake and retention of F-18 BMS-747 158–02 in cardiomyocytes: A novel PET myocardial imaging agent. J Nucl Cardiol 2007;14:782.

11. Ahmed H, Haider A, Gisler L, Schibli R, Gebhard C, Ametamey SM. [(18) F]Flurpiridaz: Facile and improved precursor synthesis for this next-generation cardiac positron emission tomography imaging agent. ChemMedChem 2020;15:1040-3.

12. Goertzen AL, Bao Q, Bergeron M, Blankemeyer E, Blinder S, Cañadas M, et al. NEMA NU 4–2008 comparison of preclinical PET imaging systems. J Nucl Med 2012;53:1300-9.

13. Krämer SD, Betzel T, Mu L, Haider A, Herde AM, Boninsegni AK, et al. Evaluation of (11)C-Me-NB1 as a potential PET radioligand for measuring GluN2B-containing NMDA receptors, drug occupancy, and receptor cross talk. J Nucl Med 2018;59:698-703.

14. Wacker CM, Wiesmann F, Bock M, Jakob P, Sandstede JJW, Lehning A, et al. Determination of regional blood volume and intra-extracapillary water exchange in human myocardium using Feruglose: First clinical results in patients with coronary artery disease. Magn Reson Med 2002;47:1013-6.

15. Logan J, Fowler JS, Volkow ND, Wolf AP, Dewey SL, Schlyer DJ, et al. Graphical analysis of reversible radioligand binding from time-activity measurements applied to [N-11C-methyl]-(-)-cocaine PET studies in human subjects. J Cereb Blood Flow Metab 1990;10:740-7.

16. Grubbs FE. Procedures for detecting outlying observations in samples. Technometrics 1969;11:1-21.

17. Sherif HM, Nekolla SG, Saraste A, Reder S, Yu M, Robinson S, et al. Simplified quantification of myocardial flow reserve with flurpiridaz F 18: Validation with microspheres in a pig model. J Nucl Med 2011;52:617-24.

18. Nekolla SG, Reder S, Saraste A, Higuchi T, Dzewas G, Preissel A, et al. Evaluation of the novel myocardial perfusion positron-emission tomography tracer 18F-BMS-747158-02. Circulation 2009;119:2333-42.

19. Wiyaporn K, Tocharoenchai C, Pusuwan P, Higuchi T, Fung GSK, Feng T, et al. Optimization of imaging protocols for myocardial blood flow (MBF) quantification with 18F-flurpiridaz PET. Phys Med 2017;42:127-34.

20. van de Hoef TP, Siebes M, Spaan JA, Piek JJ. Fundamentals in clinical coronary physiology: Why coronary flow is more important than coronary pressure. Eur Heart J 2015;36:3312-9.

21. Nekolla SG, Reder S, Saraste A, Higuchi T, Dzewas G, Preissel A, et al. Evaluation of the novel myocardial perfusion positron-emission tomography tracer 18F-BMS-747158-02: Comparison to 13N-ammonia and validation with microspheres in a pig model. Circulation 2009;119:2333-42.

22. Kadrmas D, Rust T, Lazewatsky J, Slomka P, Berman D, Di Carli M, et al. Single-scan rest-stress cardiac PET imaging with Flurpiridaz F18. J Nucl Med 2012;53:140.

23. Ametamey SM, Honer M, Schubiger PA. Molecular Imaging with PET. Chem Rev 2008;108:1501-16.

24. Bourque JM, Hanson CA, Agostini D, Bateman TM, Bax JJ, Beanlands RSB, et al. Assessing myocardial perfusion in suspected coronary artery disease: rationale and design of the second phase 3, open-label multi-center study of flurpiridaz (F-18) injection for positron emission tomography (PET) imaging. J Nucl Cardiol 2021;28:1105.

25. Packard RRS, Cooke CD, Van Train KF, Votaw JR, Sayre JW, Lazewatsky JL, et al. Development, diagnostic performance, and interobserver agreement of a (18)F-flurpiridaz PET automated perfusion quantitation system. J Nucl Cardiol 2020. https://doi.org/10.1007/s12350-020-02335-6.

26. Aljizeeri A, Badarin FA, Al-Mallah MH. Automation in nuclear cardiology: time for flurpiridaz to join the club. J Nucl Cardiol 2020. https://doi.org/10.1007/s12350-020-02421-9.

27. Maddahi J, Bengel F, Czernin J, Crane P, Dahlbom M, Schelbert H, et al. Dosimetry, biodistribution, and safety of flurpiridaz F 18 in healthy subjects undergoing rest and exercise or pharmacological stress PET myocardial perfusion imaging. J Nucl Cardiol 2019;26:2018-30.

28. Moody JB, Poitrasson-Rivière A, Hagio T, Buckley C, Weinberg RL, Corbett JR, et al. Added value of myocardial blood flow using (18)F-flurpiridaz PET to diagnose coronary artery disease: The flurpiridaz 301 trial. J Nucl Cardiol 2020;28:2313.

29. Calnon DA. Will (18)F flurpiridaz replace (82)rubidium as the most commonly used perfusion tracer for PET myocardial perfusion imaging? J Nucl Cardiol 2019;26:2031-3.

30. Berman DS, Germano G, Slomka PJ. Improvement in PET myocardial perfusion image quality and quantification with flurpiridaz F 18. J Nucl Cardiol 2012;19:S38-45.

31. Beller George A, Watson DD. A welcomed new myocardial perfusion imaging agent for positron emission tomography. Circulation 2009;119:2299-301.

32. Berman DS, Maddahi J, Tamarappoo BK, Czernin J, Taillefer R, Udelson JE, et al. Phase II safety and clinical comparison with single-photon emission computed tomography myocardial perfusion imaging for detection of coronary artery disease: flurpiridaz F 18 positron emission tomography. J Am Coll Cardiol 2013;61:469-77.

33. Maddahi J, Czernin J, Lazewatsky J, Huang S-C, Dahlbom M, Schelbert H, et al. Phase I, first-in-human study of BMS747158, a novel 18F-labeled tracer for myocardial perfusion PET: Dosimetry, biodistribution, safety, and imaging characteristics after a single injection at rest. J Nucl Med 2011;52:1490.

34. Maddahi J, Lazewatsky J, Udelson JE, Berman DS, Beanlands RSB, Heller GV, et al. Phase-III clinical trial of fluorine-18 flurpiridaz positron emission tomography for evaluation of coronary artery disease. J Am Coll Cardiol 2020;76:391-401.

35. Sharir T, Kovalski G. Absolute myocardial blood flow vs relative myocardial perfusion: Which one is better? J Nucl Cardiol 2018;25:1629-32.

36. Packard RR, Huang SC, Dahlbom M, Czernin J, Maddahi J. Absolute quantitation of myocardial blood flow in human subjects with or without myocardial ischemia using dynamic flurpiridaz F 18 PET. J Nucl Med 2014;55:1438-44.

37. Johnson NP, Gould KL. Simplified Quantification of myocardial flow reserve with 18F-Flurpiridaz: Validation with microspheres in a pig model. J Nucl Med 2011;52:1835.

38. Sherif HM, Nekolla SG, Schwaiger M. Reply: Simplified quantification of myocardial flow reserve with 18F-flurpiridaz:

Validation with microspheres in a pig model. J Nucl Med 2011;52:1835-6.

39. Saito S, Masuda K, Mori Y, Nakatani S, Yoshioka Y, Murase K. Mapping of left ventricle wall thickness in mice using 11.7-T magnetic resonance imaging. Magn Reson Imaging 2017;36:128-34.

40. Maddahi J, Packard RR. Cardiac PET perfusion tracers: Current status and future directions. Semin Nucl Med 2014;44:333-43.

41. Constantinides C, Mean R, Janssen BJ. Effects of isoflurane anesthesia on the cardiovascular function of the C57BL/6 mouse. ILAR J 2011;52:21-31.

42. Matsuda Y, Ohsaka K, Yamamoto H, Natsume K, Hirabayashi S, Kounoike M, et al. Comparison of newly developed inhalation anesthesia system and intraperitoneal anesthesia on the hemodynamic state in mice. Biol Pharm Bull 2007;30:1716-20.

43. Wu J, Bu L, Gong H, Jiang G, Li L, Ma H, et al. Effects of heart rate and anesthetic timing on high-resolution echocardiographic assessment under isoflurane anesthesia in mice. J Ultrasound Med 2010;29:1771-8.

44. Mu L, Krämer SD, Warnock GI, Haider A, Bengs S, Cartolano G, et al. [(11)C]mHED PET follows a two-tissue compartment model in mouse myocardium with norepinephrine transporter (NET)-dependent uptake, while [(18)F]LMI1195 uptake is NET-independent. EJNMMI Res 2020;10:114.